Radiolytic Hydrogen Yields in Aqueous Suspensions of Gold Particles

G. Merga,[†,‡] B. H. Milosavljevic,[†] and D. Meisel*[,†]

Radiation Laboratory and Department of Chemistry and Biochemistry, University of Notre Dame, Notre Dame, Indiana 46556, and Department of Chemistry and Biochemistry, Andrews University, Berrien Springs, Michigan 49104

Received: December 11, 2005; In Final Form: January 18, 2006

The effect of high concentrations of large gold particles, in the hundreds of nanometer size regime, on the yields of molecular hydrogen, $G(H_2)$, produced in the radiolysis of several aqueous solutions was determined. In particular we look for direct effect of radiation absorbed by the solid particles on the yield of water products. These particles, however, are catalytically active in the conversion of reducing radicals to molecular hydrogen as well. A very small increase in $G(H_2)$ observed in bromide solutions upon addition of 50 wt % of gold particles indicates that the radiolysis of the solid particles does not affect the yields in the aqueous phase. Very little exchange of charge carriers or energy between the two phases occurs in these large particle suspensions. On the other hand, efficient catalytic conversion of $(CH_3)_2C^{\bullet}OH$ radicals to H_2 is shown to occur. The efficiency of the presently studied suspensions in the redox-catalytic process is similar to that of suspensions of small particles of similar total surface area. In the presence of radicals from hydrogen atom abstraction from *tert*-butyl alcohol the yield decreases significantly, again similar to the behavior in suspensions of small particles. We conclude that the redox catalysis does not depend on the size of the particles when their size exceeds a few nanometers.

Introduction

Radiolysis of microheterogeneous systems has been a subject of considerable interest in recent years. On one hand, the study of systems that contain small particles suspended in an aqueous phase provides insight into the fundamental processes that occur inside the particles and at their interface with the medium.[1] On the other, it is also of practical interest in technological areas such as nuclear power generation and utilization, in the management of nuclear materials and their disposal, and in the application of radiation therapy.[2] Thus, much effort has been devoted to the study of radiation-initiated processes that occur at the interface of various solid particles in contact with liquids, often suspended in water.[3−5] Of particular interest in the present context are redox processes at noble-metal particle interfaces. It is now well established that metallic nanoparticles in irradiated aqueous solutions catalyze multielectron redox processes at the expense of single electron-transfer reactions.[6] Most of these studies were, however, conducted with particles of very small sizes, a few nanometers in diameter. Small nanoparticles may be highly effective as catalysts for a variety of reasons. The high surface area-to-volume ratio is an obvious contributor, but just as important might be the effect of excess surface free energy, caused by the large fraction of atoms at the surface with a multitude of dangling bonds, the high curvature of the particle surface, the preferential exposure of a particularly active phase or face of the nanocrystallites, and the presence of a phase that is unstable at bulk sizes. In the present study we determine the yields of H_2 production from irradiated aqueous suspensions of large gold particles at very high concentrations. We explore the possibility that enhanced yields result either from the transfer of charge carriers from the particles to the aqueous phase or from catalytic processes.

When each of the two phases, the aqueous phase and the solid particles, constitute a significant fraction of the total mass of the irradiated system the ionizing energy is absorbed by both phases to a significant extent. The primary outcome of the absorption of a high-energy photon, in the MeV range, is the ejection of a high-energy Compton electron. The range of this electron in various materials is large and well established.[7] However, this electron generates a large number of secondary electrons of energies in the 100 eV range. The fate of these electrons may differ from the radiolysis of either homogeneous phase alone. This is because charge carriers may cross from one phase to the other. Significantly, the density of the metals is much higher than that of water, for example 19.32 g cm^{-3} for gold. Therefore, at relatively small volumes of the metallic particles they absorb a significant fraction of the radiation. However, the fate of the energy that is absorbed in the particles is not known for most materials. Thus, we wonder if the charge carriers could escape the solid and become trapped in the aqueous phase prior to recombination or localization in the particle. Indeed, we have recently shown that charge carriers could escape from silica particles if the size of the particle is smaller than 15 nm.[8] This result was determined by measuring the yield of reduced adsorbed radicals on silica colloidal particles of increasing particle sizes produced by electrons ejected from the particles. For metals the escape probabilities are not known. It is commonly believed that a positive hole produced by the ionization rapidly annihilates by an electron from the densely populated conduction band in the metal.[7] How far can the secondary electron travel after the ionization is not known. It is possible that the distance in metals would be larger than that in insulators resulting in focusing the radiolytic effects at the particle surface.

* Address correspondence to this author. E-mail: dani@nd.edu.
[†] University of Notre Dame.
[‡] Andrews University.

10.1021/jp057231i CCC: $33.50
Published on Web 02/18/2006

Henglein and co-workers described the catalytic effects of metallic particles on radical reactions in aqueous solutions.[6,9] The initial step in these catalytic processes is often an electron-transfer reaction between the radical and the metallic particle. For strongly reducing radicals the electron-transfer step from the radical to the particle is followed by proton transfer from the aqueous phase to the charged particle, eventually leading to H_2 evolution. Other redox processes that may occur with various components of the electrolyte may compete then with proton uptake. Depending on the metal, the solution pH, and the redox potential of the radical, the number of electrons that accumulate on the particle prior to neutralization by protons varies. For instance, proton consumption follows rapidly the electron transfer on platinum, but on gold and silver a large number of electrons can accumulate before neutralization by protons commences. This ability of metals of high overpotential for the H_2 evolution reaction can be utilized to induce other redox processes, such as degradation of environmentally hazardous substances.[10] Considering the observation of high specific catalytic activity of gold particles in the few nanometer size regime for various redox processes,[11] we examine in this study radical redox catalysis on large gold nanoparticles. We find that energy (electrons) from direct ionization of these large gold particles does not escape into the aqueous phase but that the particles are highly active as redox catalysts.

Experimental Section

Suspensions of gold particles are optically opaque in the UV−vis region. Therefore, the concentration of reduced products originating from the direct ionization of the particle was measured via H_2 yield. An inline gas chromatography technique was used to determine the amount of hydrogen produced. The experimental setup consisted of a well-regulated argon stream that continuously bubbles through a sample cell made of a 1 cm quartz cuvette. A four-way valve allowed the cell to be isolated from the argon stream during the course of the radiolysis. Opening the valve directs the accumulated volatile products to a 3-m Molecular-Sieve 5A chromatographic column held at 50 °C. Products were measured with a thermal-conductivity detector. A septum for the injection of calibration gases was placed upstream from the sample cell. Gas flow through the sample was held at 40 mL min^{-1}. The retention time of H_2 under these conditions was 2.8 min.

All irradiations were performed on samples that included 2 g of water in the irradiated cuvette but the addition of gold changed the total weight of the irradiated sample. Small changes in total volume of the sample, which result from the addition of the particles, were neglected. All irradiated solutions were at natural pH (5.7−6.4), and to avoid complications no buffers were added. Some increases in pH were observed (up to pH 8.2) but it is well established that H_2 yields do not depend on pH in this range. Centrifugation at 8000 rpm for 10 min was used to precipitate the gold particles under Ar atmosphere to allow spectrophotometric measurements. Deaeration or saturation with the desired gas was achieved by bubbling the gas for 15 min through the solution prior to irradiation. UV−vis measurements were performed with a Hewlett-Packard 8453 diode-array spectrophotometer. A ^{60}Co γ-irradiator from J. L. Shepard & Associates, model 109-68, provided a dose rate of 12.5 ± 1 krad min^{-1} in water as determined by the Fricke Dosimeter. Gold powders were purchased from Alfa (radius, $r = 400-750$ nm by TEM as provided by the distributor). BET measurements performed in our laboratory yield a surface area of $S = 0.242$ m^2 g^{-1}, which translates to $r = 640$ nm. The powders were suspended in the aqueous solutions immediately prior to irradiation by vigorous stirring. Some settling of particles from the suspension was observed after about 30 min.

Results and Discussion

Mechanisms of Radiolytic Hydrogen Formation. The following well-documented reactions of hydrated electron and hydrogen atoms lead to the formation of molecular hydrogen following the radiolysis of water:[12,13]

$$2e_{aq}^- + 2H_2O \rightarrow H_2 + 2OH^- \quad (1)$$

$$e_{aq}^- + H^\bullet + H_2O \rightarrow H_2 + OH^- \quad (2)$$

$$H^\bullet + H^\bullet \rightarrow H_2 \quad (3)$$

Rate constants for these and most other reactions listed here are available in the compilation of Buxton et al.[14] Reactions 1−3 require radiolytically generated two reducing equivalents for the formation of each H_2 molecule. It should be noted that these reactions occur within the spurs prior to randomization of the primary water radiolysis fragmentation products, $<10^{-7}$ s following the absorption of the energy, as well as after their randomization. The latter fraction of primary radicals can easily be scavenged by various solutes in the bulk water. However, escape of charge carriers from the particles may lead to high local concentration of hydrated electrons near the gold-particle surface. Reaction 1−3 may then have a small contribution to the yield of hydrogen despite the high electron-scavenger concentrations in the aqueous phase (often acetone in this study).

Reactions involving the precursor to the hydrated electrons recently have been suggested to rationalize the yield of H_2 in concentrated solutions of electron scavengers.[15,16] The first step in this reaction scheme is the capture of the precursors to the hydrated electron by a water molecule to give an excited-water anion radical, H_2O^{*-}. This step is followed by ultrafast H_2 formation either directly, reaction 4,

$$H_2O^{*-} \rightarrow H_2 + O^{*-} \quad (4)$$

or via hydride formation, reactions 5 and 6.[17−20]

$$H_2O^{*-} \rightarrow H^- + OH^\bullet \quad (5)$$

$$H^- + H_2O \rightarrow H_2 + OH^- \quad (6)$$

The generation of molecular hydrogen via either pathway, reaction 4 or reactions 5 and 6, requires one radiolytic excitation/ionization event. The difficulty in scavenging this source of molecular hydrogen indicates that the process is very fast. Therefore, we chose to first measure the yield of H_2 from reactions 1−6 to test possible direct escape of reducing equivalents from the particles to the water. These fast reactions allow little time for intervention by the gold particles in the catalytic processes described later below.

The catalytic processes that convert reducing radicals to H_2 resemble the electrochemical mechanism for hydrogen evolution on metallic electrodes.[6,9] Following charging of the metallic particle by the radical, (M) and $R^\bullet$ respectively in reaction 7, charge neutralization by protons (reaction 8), and release of H_2 lead to the conversion of reducing equivalents to hydrogen (reaction 9).

$$R^{\bullet} + (M) \rightarrow (M)^{-} + R^{+} \quad (7)$$

$$H_2O + (M)^{-} \rightarrow H_{(ads)} + OH^{-} \quad (8)$$

$$2H_{(ads)} \rightarrow H_2 \quad (9)$$

Thus, two reducing radicals lead to the generation of one H_2 molecule in this sequence of reactions. The H atoms that are produced by the irradiation of water lead to H_2 in the presence of alcohols, reaction 10. This hydrogen abstraction reaction then leads to the formation of H_2 from a single hydrogen atom. The

$$H^{\bullet} + RH \rightarrow H_2 + R^{\bullet} \quad (10)$$

α-hydroxy radical, $R^{\bullet}$ (1-hydroxy-1-methylethyl radical in the present study), may further charge the particle via reaction 7, depending on the specific radical. We used the sequence of reactions 7−10 to determine the activity of the particles in the catalytic cycle.

Direct Hydrogen Formation. Figure 1 shows the amount of hydrogen gas produced in the radiolysis of deaerated 1×10^{-3} M NaBr aqueous solution vs absorbed dose, at a dose rate of 12.5 krad min^{-1}. The amount of H_2 depends linearly on the dose. The yield of hydrogen, $G(H_2) = 0.53$ molecules per 100 eV, calculated from the slope is in a good agreement with published data.[21] The linear dependence of the amount of H_2 generated on dose was maintained at least up to doses of 3 Mrad. This linear dependence indicates that a high enough steady-state concentration of bromine is maintained during the irradiation to scavenge all reducing radicals that might otherwise generate H_2 via postspur reactions 1−3. It also ensures that the hydroxyl radicals react with bromide rather than with H atoms or H_2, which otherwise would reduce the observed yield of H_2. An outline of the reaction scheme of the radiolysis of deaerated Br^{-} solutions is given by reactions 11−16:[22,23]

$$OH^{\bullet} + Br^{-} \leftrightarrow BrOH^{-} \quad (11)$$

$$BrOH^{-} + H^{+} \rightarrow Br + H_2O \quad (12)$$

$$Br\ (\text{or}\ BrOH^{-}) + Br^{-} \rightarrow Br_2^{-}\ (+ OH^{-}) \quad (13)$$

$$2Br_2^{-} \rightarrow Br_3^{-} + Br^{-} \quad (14)$$

$$e_{aq}^{-}\ (\text{or H}) + Br_3^{-} \rightarrow Br_2^{-} + Br^{-}\ (+ H^{+}) \quad (15)$$

$$e_{aq}^{-}\ (\text{or H}) + Br_2^{-} \rightarrow 2Br^{-}\ (+ H^{+}) \quad (16)$$

Bromide is oxidized in reactions 11−13 but is recovered in reaction 15−16. Thus, a steady state of bromine is established in the course of the irradiation. Bromine might further hydrolyze and disproportionate,[24] generating BrO^{-}, which would replace bromine in reactions 15 and 16. However, using ion chromatography we were unable to detect any changes in the concentration of bromide after 3 Mrad of absorbed dose. Therefore, the steady-state level of bromine and higher oxidation state species that is generated following the irradiation must be below the 1% accuracy of the instrument, i.e., below 10^{-5} M oxidized bromide. This concentration is clearly too low to interfere with spur reactions. A similar conclusion was recently reported for H_2 production in porous silica.[5] H_2 in this system is thus produced in the very fast reactions discussed in the previous section.

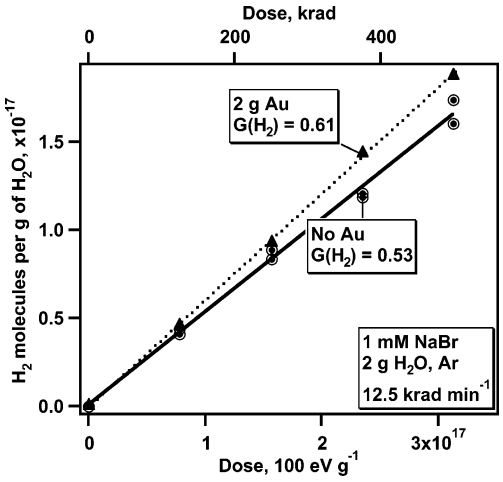

Figure 1. H_2 generation in bromide solutions (circles) and in the presence of 2 g of gold particles (triangles). Experimental conditions are shown in the figure. Only radiation absorbed by the water is included in the dose shown.

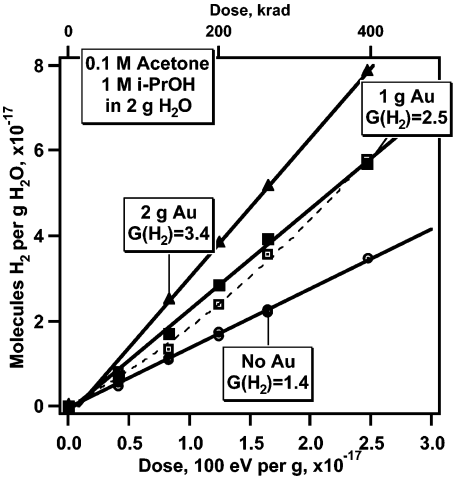

Figure 2. Yield of H_2 from irradiation of deaerated 0.1 M acetone and 1.0 M 2-propanol solutions in the absence (circles) and presence of gold particles (squares 1 g; triangles 2 g). The dose rate is 12.5 krad min^{-1}, except 0.26 krad min^{-1} for open squares. Doses are calculated assuming that only water absorbs the radiation.

The bromide solution is, therefore, an ideal system to determine the contribution of direct absorption of radiation by gold particles to the effects of water radiolysis. Figure 1 also shows the yield of H_2 from the same solution in the presence of gold particles. In a suspension of 50 wt % of gold particles (2 g each, solution and particles) $G(H_2) = 0.61$ molecules per 100 eV was measured. The small increase, $\Delta G(H_2) = 0.08$, is above the error limits of the measurements and may reflect a small "direct effect" in the radiolysis of the metal particles. A fraction of the ionization events within the gold particles may lead to electrons ejected into the aqueous phase in the vicinity of the surface and these can be trapped in the water and participate in the formation of hydrogen. However, the total dose absorbed by the sample is twice that in the aqueous solution in the absence of particles. Therefore, we may conclude that the exchange of energy between the two phases is rather small with these relatively large particles. Upon a similar loading of the suspension with small silica particles the yield of reducing radicals doubles.[25]

Catalytic H_2 Production. Figure 2 shows the dependence of the amount of H_2 generated from deaerated aqueous solutions containing 0.1 M acetone and 1 M 2-propanol on dose. At the

concentrations used the hydrated electron reacts predominantly with acetone, while the hydroxyl radical reacts with 2-propanol to yield the same 1-hydroxy-1-methylethyl radical:

$$e_{aq}^- + (CH_3)_2CO\ (+ H^+) \rightarrow (CH_3)_2C^{\bullet}OH \qquad (17)$$

$$OH^{\bullet} + (CH_3)_2CHOH \rightarrow (CH_3)_2C^{\bullet}OH + H_2O \qquad (18)$$

Similarly, the radiolytically produced primary hydrogen atom abstracts another H atom to yield yet another 2-propanol radical along with molecular hydrogen:

$$H^{\bullet} + (CH_3)_2CHOH \rightarrow (CH_3)_2C^{\bullet}OH + H_2 \qquad (19)$$

The organic radicals undergo radical−radical combination reactions in the absence of the metallic particles. The yield of H_2 in the absence of gold particles is then expected to be

$$G(H_2) = G(H_2)_0 + G(H) = 0.55 + 0.6 = 1.15 \text{ molecules per 100 eV}$$

where $G(H_2)_0$ is the yield observed in the absence of the alcohol, e.g., in the bromide solutions described above. A somewhat higher yield, $G(H_2) = 1.45$ molecules per 100 eV was measured, which can be attributed to the high alcohol and acetone concentrations. At these concentrations, where $k[S] > 10^8\ s^{-1}$, the scavenger, S, intervenes with early spur reactions and the observed yields are higher than in dilute solutions. As can be seen in Figure 2 the concentration of the radiation produced hydrogen linearly depends on absorbed dose indicating that the yield does not change up to doses of at least 0.5 Mrad.

The radical, R$^{\bullet}$, from 2-propanol is a strongly reducing radical ($E^\circ = -1.89$ V vs NHE),[26] capable of generating H_2 provided a redox catalyst is available (reactions 7−9). Because the sole source of hydrogen in the system is water or organic solutes, only the dose absorbed by water is taken into account in the calculation of absorbed dose in Figures 1, as well as in Figure 2. However, the dose absorbed by the whole sample is doubled when the weight of Au particles equals that of H_2O. In the absence of any interaction between the two phases the yield of H_2 will remain unchanged upon the addition of the solid particles. Clearly, as seen in Figure 2, the yield of hydrogen increases upon increasing the concentration of gold.

As discussed earlier, two possible types of interactions may explain this increase in yield. Either energy that is absorbed by the gold particles escapes into the aqueous phase, or the particles catalyze the hydrogen evolution reaction as summarized in reactions 7−9. The preceding section shows that the former does not occur on the very fast time scale, and therefore, we conclude that the catalytic processes are very efficient even in these large-particle suspensions. It is, however, noteworthy that the increase in yield follows the increase in the absorbed dose in the whole sample. As Figure 3 indicates, if one assumes that all of the dose that is absorbed by the sample can contribute to the yield of H_2, the yield hardly changes upon increasing the Au concentration. Nonetheless, in view of the results from the bromide system (Figure 1) we believe that this correlation is fortuitous. The yield of the radicals does not increase but their conversion to hydrogen becomes more efficient with the addition of the catalyst. In that case the dependence on gold concentration indicates competition between the catalytic conversion of the radicals to hydrogen, another reaction that does not produce hydrogen and does not involve participation of the particles.

Possible nonproductive competing reactions are recombination of the radicals and possibly a reaction with residual oxygen

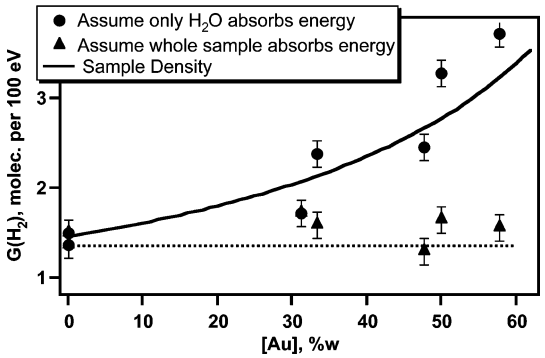

Figure 3. Yield of H_2 from irradiated Au suspensions. Experimental conditions are as in Figure 2: (triangles) dose calculated assuming total absorbed dose by the sample contributes to H_2 formation; (circles) only dose absorbed by water contributes.

or other impurity at the submicromolar level of concentration.[9] Close examination of Figure 2 indicates that both are competing in this system. As can be seen in Figure 2 (compare solid to open squares in Figure 2) the yield of H_2 decreases at a low dose rate relative to the yield at the higher dose rate. Contrary to commonly observed dose-rate dependence, this behavior cannot be due to a radical−radical recombination reaction. The latter would become more dominant at the higher dose rate and the yield would then decrease. Furthermore, this dose-rate dependence is eliminated at higher doses. At doses larger than 250 krad (1.7×10^{19} eV g^{-1}) the yield is independent of dose rate. We tentatively assign the dose-rate dependence to a competition of the catalytic reaction with small concentrations of impurities, probably oxygen or gold ions at the particle surface. As the total absorbed dose increases the impurity is eliminated from the system. On the other hand, the dependence on gold concentration is attributed to competition of the charge-transfer reaction to the particle (reaction 7) with the radical recombination reaction in the bulk. With this assumption we estimate below the rate of the radicals with the particles.

At complete catalytic conversion of the 1-hydroxy-1-methylethyl radicals, the total H_2 yield expected from the mechanism described above in the particle suspensions is

$$G(H_2) = G(H_2)_0 + G(H) + {}^1/_2\{0.85[G(e_{aq}^-) + G(OH)] + G(H)\} - G(H_2O_2) = 0.55 + 0.6 - 0.8 + \{2.4 + 2.4 + 0.6\}/2 = 3.05 \text{ molecules per 100 eV}$$

This calculated yield assumes, as sometimes observed, that the radiolytically produced H_2O_2 preferentially reacts with the charged metallic particles in a two-electron-transfer reaction at the overpotential required for hydrogen evolution.[6] It also takes into account the partial, 85% of the OH radical, production of the 1-hydroxy-1-methylethyl radicals in reaction 18.[29] The yield may further decrease if the residual 15% of 2-hydroxy-2-methylethyl radicals oxidizes the charged gold particles. On the other hand, the high concentration of 2-propanol and acetone usually leads to some increase in the yield.

The yield of H_2 is essentially the predicted one at 50 wt % of Au. However, at 33 wt % of gold (1.0 g of Au) the yield is approximately 80% of the predicted total H_2 yield and thus the same percentage of R$^{\bullet}$ react with the particles to generate H_2. From the dose rate (12.5 krad min^{-1}), the yield of R$^{\bullet}$ (6.2 radicals per 100 eV), and the rate constant for the radical recombination ($k = 1 \times 10^9$ M^{-1} s^{-1}), one calculates a steady-state concentration of $[R^{\bullet}]_{ss} = 2.5 \times 10^{-8}$ M in the absence of

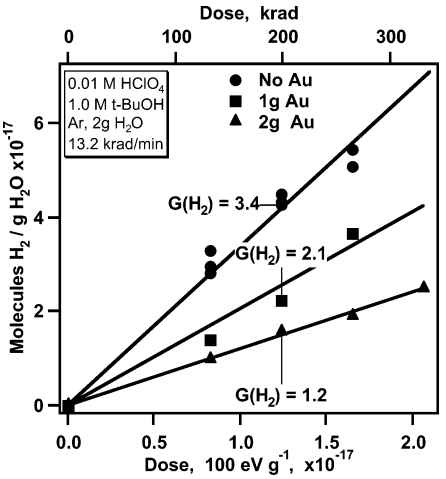

Figure 4. Yield of H_2 from irradiation of deaerated acidic solutions containing *tert*-butyl alcohol at pH 2. Experimental conditions shown in the figure. The dose was calculated assuming only water absorbs the energy to produce H_2.

gold. For the competition between the reaction of the radicals with gold and their recombination reaction we used the IBM Kinetic Simulator to numerically calculate the rate at which 80% of the radicals react with the particles. This yields $k = 90\ s^{-1}$ for reaction 7 in the presence of 1.0 g of Au. At this loading of Au the concentration of particles is approximately 6.5×10^{-12} M and thus $k_7 \sim 1.4 \times 10^{13}\ M^{-1}\ s^{-1}$. This rate constant is within the expected range for diffusion-controlled rate constant for particles of $r = 640$ nm, 3 orders of magnitude larger than the reaction radius for molecular collisions.

The high rate of the 1-hydroxy-1-methylethyl radical reaction with the gold particles indicates that to obtain the observed high H_2 yields the rate of the electron-transfer step in the catalytic hydrogen evolution needs to be close to the diffusion-controlled limit. In the scheme proposed by reactions 7−9 this conclusion infers that the rate of consumption of protons (reaction 8) and the rate of release of adsorbed hydrogen atoms are high enough so the net rate of H_2 evolution is determined by the rate that electrons can be supplied to the particle to maintain high enough overpotential (reaction 7). It has been shown earlier that the rate of electron transfer from the same radicals to silver, gold, and platinum particles is essentially diffusion controlled but the rate of consumption of protons is slower until high enough overpotential is obtained on the metallic particles.[27,28] The present results indicate that a high overpotential is maintained on the large Au particles as well, from relatively early stages of the irradiation. Under these conditions reducing the overpotential for the hydrogen evolution reaction, e.g., by changing the identity of the metal catalyst, cannot accelerate the catalytic process any further.

In considering again the possible effects of direct absorption of radiation by the gold particles, further verification that the 1-hydroxy-1-methylethyl radical concentration does not increase upon increasing the loading with particles is obtained from irradiation of similar solutions that contain 1×10^{-2} M methyl viologen (MV^{2+}) in the pH range of 4.6−9.0. Under these experimental conditions the alcohol radicals reduce the viologen to the MV^+ radical but the production of H_2 by the latter is very slow because of the relatively high pH. Under these conditions $G(H_2) = 1.20 \pm 0.15$ was measured even in the presence of 50 wt % of gold, corresponding to the uncatalyzed yield. Direct observation of the well-known UV−vis absorption of the MV^+ radical requires precipitation and separation of the gold particles from the suspension. Following centrifugation under deaerated conditions and then measuring the yield of MV^+ radicals we obtain 6.0 ± 1.0 close to the expected yield of the radicals from 2-propanol. The large error in these measurements reflects the difficulties encountered in measuring the optical absorption following centrifugation under deaeration.

Catalytic Oxidation Reactions. In contrast to the 1-hydroxy-1-methylethyl radical from 2-propanol obtained in reactions 18 and 19, the analogous hydrogen abstraction reactions with *tert*-butyl alcohol generate an oxidizing radical.[29] The latter alcohol is often used as an OH scavenger to generate a relatively inert radical. We, therefore, tested the effect of the gold particles on yields in the presence of *tert*-butyl alcohol. Figure 4 shows the yield of hydrogen versus dose from deaerated solutions containing 0.01 M $HClO_4$ and 1 M *tert*-butyl alcohol. Reactions 18a, 19a, and 20 then describe the fate of the primary intermediates of the water radiolysis:

$$OH^\bullet + (CH_3)_3COH \rightarrow (CH_3)_2(CH_2^\bullet)COH + H_2O \quad (18a)$$

$$(e_{aq})^- + H^+ \rightarrow H^\bullet \quad (20)$$

$$H^\bullet + (CH_3)_3COH \rightarrow (CH_3)_2(CH_2^\bullet)COH + H_2 \quad (19a)$$

The expected yield of H_2 in the absence of the metallic particles is

$$G(H_2)_{tot} = G(H_2)_0 + G(H) + G(e_{aq}^-) = 3.95 \text{ molecules per } 100 \text{ eV}$$

The observed yield of hydrogen formation is 3.4, somewhat lower but reasonably close to the expected value. This suggests that the hydrogen abstraction, reaction 19a, dominates the reactions of H atoms, even though approximately 15% are lost to radical−radical reactions. This loss results from the relatively slow abstraction reaction ($k_{19a} = 1.7 \times 10^5\ M^{-1}\ s^{-1}$).

As can be seen in Figure 4 the presence of gold particles reduces the yield of molecular hydrogen significantly. Several processes may contribute to this reduction in yield. Because of the slow rate of reaction 19a, reduction of the *tert*-butyl alcohol radicals produced by OH (in reaction 18a) by $H^\bullet$ atoms, or excess electrons, on the gold particles (reaction 21) becomes feasible.

$$(CH_3)_2(CH_2^\bullet)COH + (Au)_p^- + H^+ \text{ (or } H_{ads}) \rightarrow (CH_3)_3COH \quad (21)$$

This sequence of reactions then amounts to catalyzed recombination of the H atoms with the radicals from the alcohol. When all $H^\bullet$ atoms react along this pathway the H_2 yield should decrease to 0.55 molecule per 100 eV but this could not be observed at the highest concentrations of alcohol and gold used in this study. Other processes that may contribute to the reduction in yield include catalyzed consumption of *tert*-butyl alcohol radicals by the hydrolyzed alcohol. It is well established that tertiary alcohols dehydrate relatively easily in acidic aqueous solutions:

$$(CH_3)_3COH \rightarrow (CH_3)_2C{=}CH_2 + H_2O \quad (22)$$

Addition of the H atom to the double bond created in reaction 22 then becomes a viable pathway for their consumption.[30] However, it should be emphasized that either the dehydration reaction or the addition to the double bond must be catalyzed

by the metallic particles to contribute to the reduced yield observed in this study.

Conclusion

Two issues were addressed in this study: the possible escape of radiolytically produced charge carriers from the gold particles and the catalytic activity of the particles. Experiments on the yield of H_2 that is generated in the fast time regime indicate that no reducing carriers escape from the particles to contribute to that yield. However, since the efficiency of escape may depend on the size of the particles and relatively large particles were utilized in this study, possible escape of carriers from smaller particles remains possible. Escape of carriers from smaller metallic particles is now under investigation. On the other hand, the large metallic particles appear to be catalytically active in the conversion of reducing radicals to hydrogen. Since essentially complete conversion of the radicals to hydrogen is observed we conclude that the presently utilized particles are as efficient as the smaller particles studied in suspension. Of course, the conversion to hydrogen in the large particles requires much larger quantity of catalyst because of the smaller particle concentration and their smaller specific surface area.

Acknowledgment. Support by the U.S. Department of Energy Office of Basic Energy Sciences is gratefully acknowledged. This is document NDRL No. 4509 from the Notre Dame Radiation Laboratory.

References and Notes

(1) (a) Grigoriev, E.; Trakhtenberg, L. *Radiation Chemical Processes in Solid Phase. Theory and Applications*; CRC Press: Boca Raton, FL, 1996; Chapter 8, p 161. (b) Meisel, D. In *Nanoscale Materials*; Liz-Marzan, L., Kamat, P., Eds.; Kluwer Publishers: New York, 2003; pp 119−134.

(2) (a) Orlando, T. M.; Meisel, D. In *Nuclear Site Remediation*; Eller, G., Heinman, W., Eds.; ACS Symp. Ser. No. 778; American CHemical Society: Washington, DC, 2001; pp 284−296. (b) Hainfeld, J.; Slatkin, D.; Smilowitz, H. *Phys. Med. Biol.* **2004**, *49*, N309

(3) Aleksandrov, A. B.; Yu Bychkov, A.; Vall, A. I.; Petrik, N. G.; Sedov, V. M. *Zh. Fiz. Khim.* **1991**, *65*, 1604.

(4) (a) Petrik, N. G.; Alexandrov, A. B.; Vall, A. I. *J. Phys. Chem. B* **2001**, *105*, 5935. (b) Thomas, J. K. *Chem. Rev.* **1993**, *93*, 301.

(5) (a) Foley, S.; Rotureau, P.; Pin, S.; Baldacchino, G.; Renault, J. P.; Mialocq, J. C. *Angew. Chem., Int. Ed.* **2005**, *44*, 110. (b) Rotureau, P.; Renault, J. P.; Lebeau, B.; Patarin, J.; Mialocq, J. C. *ChemPhysChem.* **2005**, *6*, 1316.

(6) Henglein, A. *Top. Curr. Chem.* **1988**, *143*, 113.

(7) Spinks, J. W.; Woods, R. J. *An Introduction to Radiation Chemistry*, 3rd ed.; J. Wiley & Sons: New York, 1990.

(8) Milosavljevic, B. H.; Pimblott, S. M.; Meisel, D. *J. Phys. Chem. B* **2004**, *108*, 6996

(9) Westerhausen, J.; Henglein, A.; Lilie, J. *Ber. Bunsen-Ges. Phys. Chem.* **1981**, *85*, 182.

(10) Subramanian, V.; Wolf, E. E.; Kamat, P. V. *J. Am. Chem. Soc.* **2004**, *126*, 4943.

(11) Haruta, M.; Tsubota, S.; Kobayashi, T.; Kageyama, H.; Genet, M. J.; Delmon, B. *J. Catal.* **1993**, *144*, 175.

(12) Draganic, Z. D.; Draganic, I. G. *J. Phys. Chem.* **1971**, *75*, 3950.

(13) Peled, E.; Czapski, G. J. *J. Phys. Chem.* **1970**, *74*, 2903.

(14) Buxton, G. V.; Greenstock, C. L.; Helman, W. P.; Ross, A. B. *J. Phys. Chem. Ref. Data* **1988**, *17*, 513.

(15) Pastina, B.; LaVerne, J. A.; Pimblott, S. M. *J. Phys. Chem. A* **1999**, *103*, 5841.

(16) LaVerne, J. A.; Pimblott, S. M. *J. Phys. Chem. A* **2000**, *104*, 9820.

(17) Kimmel, G. A.; Orlando, T. M.; Vezina, C.; Sanche, L. *J. Chem. Phys.* **1994**, *101*, 3282.

(18) Curtis, M. G.; Walker, I. C. *J. Chem. Soc., Faraday Trans.* **1992**, *88*, 2805.

(19) Melton, C. E. *J. Chem. Phys.* **1972**, *57*, 4218.

(20) Cobut, V.; Jay-Gerin, J.-P.; Frongillo, Y.; Patau, J. P. *Radiat. Phys. Chem.* **1996**, *47*, 247.

(21) LaVerne, J. A. *J. Phys. Chem.* **1988**, *92*, 2808.

(22) Behar, D. *J. Phys. Chem.* **1977**, *81*, 1447.

(23) (a) Mamou, A.; Rabani, J.; Behar, D. *J. Phys. Chem.* **1977**, *81*, 1447. (b) D'Angelantonio, M.; Venturi, M.; Mulazzani, Q. G. *Radiat. Phys. Chem.* **1988**, *32*, 319.

(24) Beckwith, R. C.; Wang, T. X.; Margerum, D. W. *Inorg. Chem.* **1996**, *35*, 995.

(25) Schatz, T.; Cook, A. R.; Meisel, D. *J. Phys. Chem.* **1998**, *102*, 7225.

(26) Wardman, P. *J. Phys. Chem. Ref. Data* **1989**, *18*, 1637.

(27) Meisel, D.; Mulac, W. A.; Matheson, M. S. *J. Phys. Chem.* **1981**, *85*, 179.

(28) Matheson, M. S.; Lee, P. C.; Meisel, D.; Pelizzetti, E. *J. Phys. Chem.* **1983**, *87*, 394.

(29) Asmus, K.-D.; Mockel, H.; Henglein, A. *J. Phys. Chem.* **1973**, *77*, 1218.

(30) Alam, M. S.; Janata, E. *Chem. Phys. Lett.* **2004**, *398*, 557.